JTTEE5 4:59-66

Comparison of Plasma-Sprayed Alumina Coatings by RF and DC Plasma Spraying

L. Bianchi, A. Grimaud, F. Blein, P. Lucchèse, and P. Fauchais

Splat size and shape-factor distributions for plasma-sprayed alumina particles on various substrates were studied using a setup derived from the line-scan test. Direct-current (dc) and radiofrequency (rf) plasma torches were used to study the influence of particle velocity at impact. The influence of substrate temperature prior to spraying also was studied. Splats collected on smooth substrates kept below 100 °C were extensively fingered and had poor substrate contact. When the substrates were heated to 300 °C before spraying, the splats became disk-shaped and their substrate contact was very good. Similar results were obtained for rough substrates. Coating adhesion decreased with particle velocity and was lower for the dc plasma torch when using larger particles, which did not melt as well as smaller ones. Melting and adhesion were much improved with the rf torch.

1. Introduction

MANY studies have been devoted to plasma jets produced either by direct current (dc) arcs (Ref 1) or by radiofrequency (rf) plasma torches (Ref 2) and to particles in flight (Ref 3, 4), but few have considered coating formation. Coating properties strongly depend on the nature and roughness of the substrate, its oxidation state, its temperature, and the molten particle velocity at impact; the influence of these different parameters is not yet clearly understood (Ref 5-9). An important coating property is adhesion integrity, which is linked to the contacts between the splats and the substrate and/or the previously deposited layers. This contact can represent less than 20% of the surface of the splat, as emphasized by McPherson (Ref 10), and any improvement of it significantly influences coating adhesion. The aim of this paper is to link the flattening of alumina particles to the resulting mechanical properties of the coating.

The splats, collected on flat substrates, were studied by a method derived from the line-scan test (Ref 11), which allowed determination of their diameter and shape distributions with respect to substrate temperature and surface roughness as well as their position in the spray cone. To study the influence of particle velocity at impact, three torches (two dc and one rf) were used, allowing the velocity of fused and crushed alumina particles (– 45+22 μm) to be varied from 60 to 250 m/s. The influence of the particle molten state was also studied by spraying larger particles (–90+45 μm).

Keywords: adhesion, cooling rate, particle diagnostics, shape factor, splat formation, thermal contact

L. Bianchi, F. Blein, and **P. Lucchèse,** CEA/DAM BIII, Bruyères le chatel, France; **A. Grimaud** and **P. Fauchais,** L.M.C.T.S., IRA320 CNRS—Equipe Plasma, Laser, Matériaux, University of Limoges, Science Faculty, Limoges, France

2. Experimental Procedure and Coating Production

2.1 *Spraying Conditions*

Two conventional dc plasma torches, both designed in the laboratory, were used for atmospheric plasma spraying (APS) (Ref 12). One had a 7 mm internal diameter (ID) nozzle, the other a 10 mm ID nozzle (to allow reduced particle velocities). The same plasma gas flow rates (45 slm Ar, 15 slm H_2) and arc current (600 A) were used for both torches, and the powder carrier gas flow rate was adjusted so that the mean particle trajectory made a 3.3° angle with the torch axis.

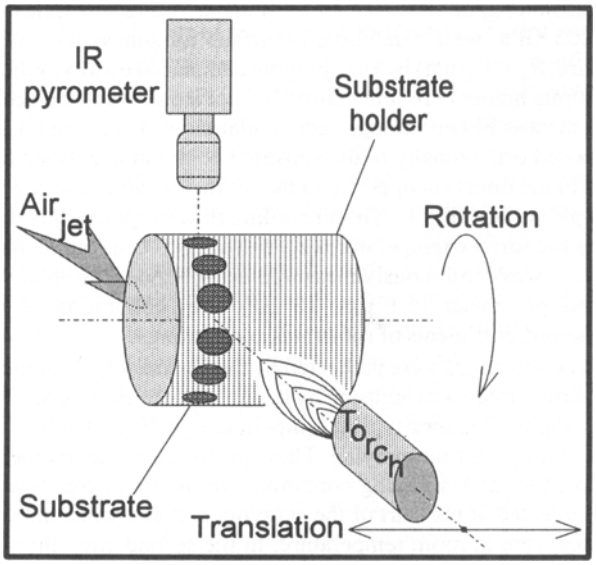

Fig. 1 Experimental set up for plasma deposition

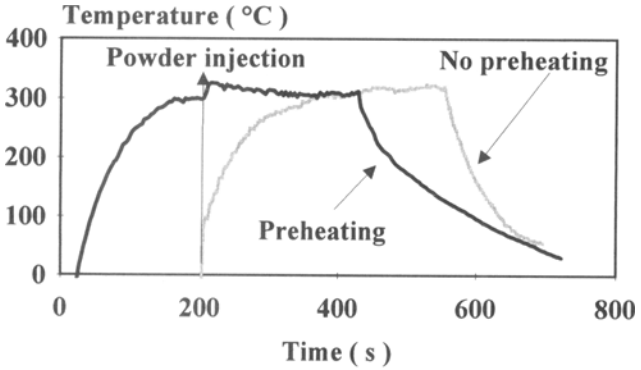

Fig. 2 Substrate and coating temperature evolution during spraying with and without preheating

Inductive plasma spraying (IPS) with an rf plasma torch TEKNA PL 50 (TEKNA Plasma Systems Inc., Sherbrooke, Quebec, Canada) (Ref 13), was also performed at a chamber pressure of 4.8×10^4 Pa. The rf plasma torch consisted of a water-cooled 50 mm ID ceramic confinement tube surrounded by a four-turn induction coil connected to the power supply. It typically worked at a 3 MHz frequency for a plate power below 60 kW (47 kW in our study), with 50 slm Ar as central gas and 90 slm Ar plus 10 slm H_2 as sheath gas. For more details on the spraying parameters, see Ref 14 and 15.

2.2 *Coating Production*

Fused and crushed alumina particles (–45+22 μm) were sprayed with the two dc plasma torches and the rf torch. Particles with a larger size distribution (–90+45 μm), which were more difficult to melt, were sprayed with the 10 mm ID nozzle and the rf plasma torch. The same experimental setup was used (Ref 16) for APS and IPS to achieve a reliable comparison of the various deposits.

The disk-shaped samples (25 mm diam, 4 mm thick), made of type 304L stainless steel with a linear coefficient of thermal expansion (α) of 18×10^{-6} m/m · K and a Young's modulus (E) of 203 GPa, were sandblasted (surface roughness root mean square, $R_a \approx 12$ mm) before spraying and placed on a cylindrical substrate holder (110 mm diam). To cool the substrate and coating, air was blown through rectangular slots (1×28 mm^2) and disposed orthogonally to the substrate holder at a distance of 5 mm in the direction opposite to the plasma jet and covering the sample surface (Fig 1). The air cooling flow rate was adjusted to keep the surface temperature (T_s) below 350 °C during deposition. T_s was continuously measured using a monochromatic infrared pyrometer (5.1 μm, 10 Hz) after calibration of the emission coefficients of substrates and coatings.

The substrates were preheated by the plasma jet; the preheating temperature was adjusted by controlling the cooling air flow rate. Figure 2 shows typical temperature profiles of substrates and coatings during spraying. These profiles were nearly identical for the three spraying conditions. In the first case, powder was injected at the start of the spraying process, when the substrates were at room temperature. In the second case, the substrates were preheated to 300 °C with the plasma torch before powder injection. When the powder was injected after preheating, with a feed rate of 1 kg/h, T_s increased by about 50 °C when the cooling air flow rate was not modified. On spraying to the required coating thickness (≈0.3 mm), the plasma jet and the cooling air jets were turned off to allow the coating and substrate to cool slowly while the substrate holder continued to rotate. The temperature of 300 °C was chosen in order to obtain disk-shaped splats (Ref 14). Below 150 °C, the splats were extensively fingered. The translation velocity of the torch was 24 mm/s for the three spraying conditions, and the rotation of the substrate holder was adjusted to achieve a 50% bead overlap.

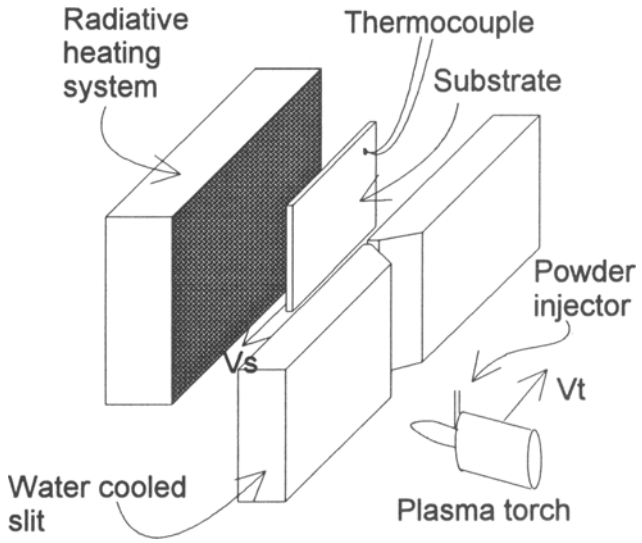

Fig 3. Experimental setup to collect individual splats

2.3 *Deposit Characterization*

An experimental setup, derived from the line-scan test (Ref 11), was developed to collect individual splats without overlapping and to isolate the substrate from the plasma thermal flux. The system consisted of a type 304L stainless steel substrate ($110 \times 100 \times 3$ mm^3) placed behind two water-cooled screens forming a 2 mm wide slit and translated in the direction opposite to the spray gun displacement (see Fig. 3). A controlled radiation heating system was placed behind the substrate, the temperature of which was monitored through use of a thermocouple. Observation of the collected splats by optical microscopy coupled with image analysis (Ref 14, 16) produced statistical information on splat shape factor, diameter, and location in the spray cone.

Coating hardness was evaluated with a 5 N load applied for 30 s, and 20 measurements on the coating cross section were performed for each spraying condition. Coating adhesion was measured according to test DIN 50150; five tests were carried out for each spraying condition. Density was measured using the water-displacement method after removal of the deposits by acid dissolution of the substrate. Microstructure was evaluated by optical and scanning electron microscopy (SEM). Splat profiles were measured using a profilometer with a load of 5×10^{-4} N.

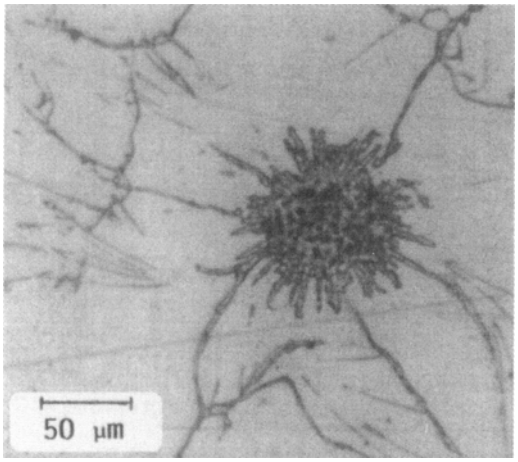

(a)

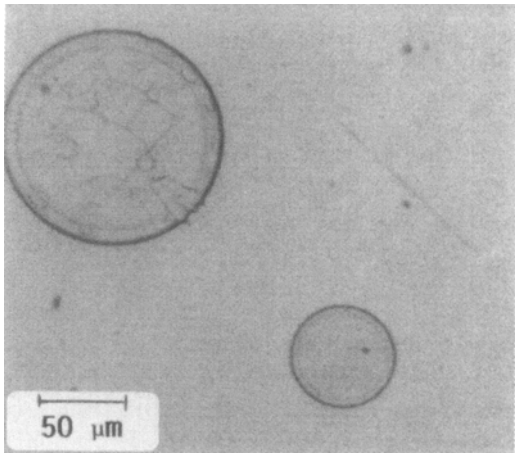

(b)

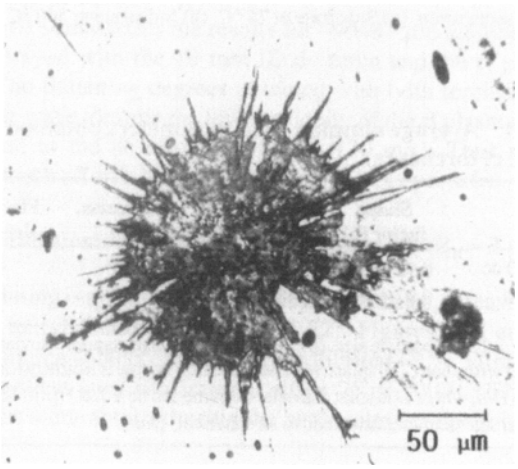

(c)

Fig 4. Alumina splats collected on a steel substrate for particles sprayed with the 7 mm ID nozzle dc plasma torch. (a) Substrate at 75 °C. (b) Substrate at 300 °C. (c) Substrate at 400 °C

3. Results and Discussion

3.1 *Influence of Substrate Temperature and Particle Velocity on Splat Formation*

3.1.1 Smooth Stainless Steel Substrates ($R_a \approx 0.1$ mm)

A low particle velocity during spraying generally produces almost lenticular splats (Ref 2). However, as indicated by the following results, this statement must be modified when considering the influence of substrate temperature, as shown in Fig. 4 for particles sprayed with the 7 mm ID nozzle dc plasma torch. In this case, the mean particle velocity for the –45+22 μm alumina particles was close to 250 m/s. Indeed, very distorted splats (Fig. 4a) formed on a cold substrate (T_s = 75 °C), as confirmed by the corresponding shape factor (SF) distribution (Fig. 5a), with a mean value of 0.55 ± 0.16. The morphology of particles sprayed on hot substrates (T_s = 300 °C), however, changed drastically to become lenticular (Fig. 4b), with a shape factor close to 1 (SF = 0.92 ± 0.12) (Fig. 5b). It is worth noting that, with a hot substrate, even the particles collected on the fringes of the spray cone had a lenticular shape with almost the same shape factor as those collected in the center of the spray cone. When T_s increased to 400 °C (Fig. 4c), the splats exhibited a morphology similar to that formed at T_s = 75 °C, with very distorted shapes. This was probably due to the oxide layer formed at the substrate/coating interface.

This general behavior regarding splat morphology evolution versus T_s also occurred when the particle velocity at impact was very low, about 60 m/s with IPS. Figures 6(a) and (b) show alumina splats obtained with the rf plasma torch for two substrate temperatures. At a low substrate temperature (75 °C), droplets of splashed material were visible and the collected splats were more distorted (Fig. 6a) than those obtained with the 7 mm ID nozzle dc plasma torch, although the particle velocity at impact in the latter case was more than five times lower. One possible explanation (Ref 17) is that when splat thickness increases and/or when contact with the substrate becomes poor due to lower impact velocity, the cooling rate decreases significantly. Thus, the upper part of the liquid material has a longer cooling time and exhibits enhanced flow. For this temperature condition, only a few splats were collected because of their poor adhesion to the substrate. It was impossible to perform a statistical study of their shape and diameter evolution.

For T_s = 300 °C, the only noticeable difference from the splats sprayed with the 7 mm ID nozzle plasma torch on a substrate at the same temperature (compare Fig. 4b and 6b) was their thickness, which was much greater in the case of IPS, with a correspondingly lower mean diameter and thus lower flattening degree (see Table 1). The shape factor distribution (Fig. 7) showed a slightly higher mean value (about 0.97) than that measured for the particles sprayed with the 7 mm ID nozzle plasma torch, probably due to the lower particle velocity at impact.

As shown by the cooling rate measurements of zirconia particles impacting on hot, nonoxidized, smooth substrates (Ref 17), the contact between the splat and the substrate increases when particle velocity increases, at least for particles with similar heat treatments. The microcrack network that results from

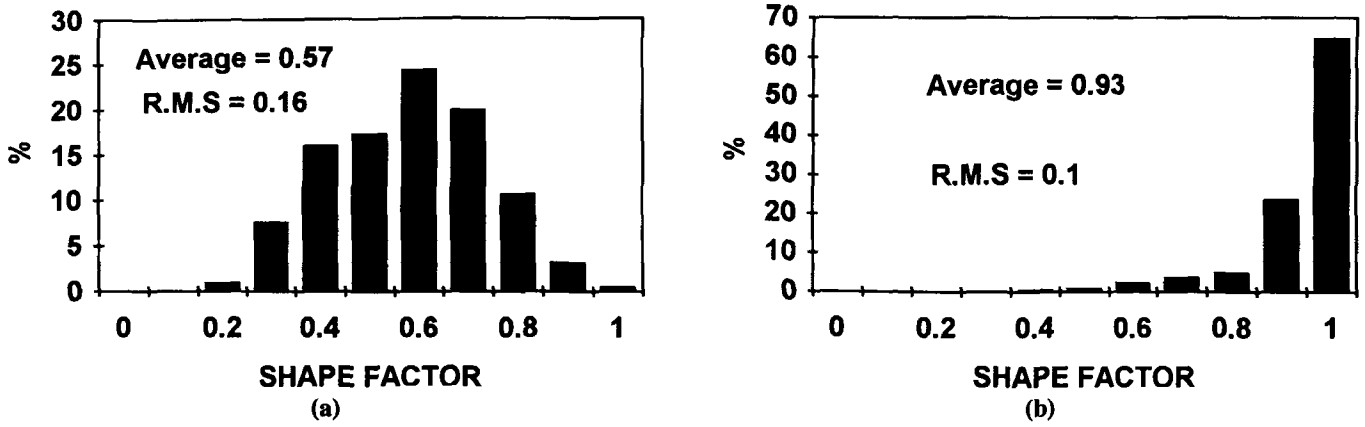

Fig 5. Shape factor distribution for alumina splats on steel substrate for particles sprayed with the 7 mm ID nozzle dc plasma torch. The shape factor is a dimensionless unit equal to $(1/4\pi)(P^2/S)$, where P is the splat perimeter (μm) and S is the splat surface (μm^2). R.M.S., root mean square. (a) Substrate at 75 °C. (b) Substrate at 300 °C

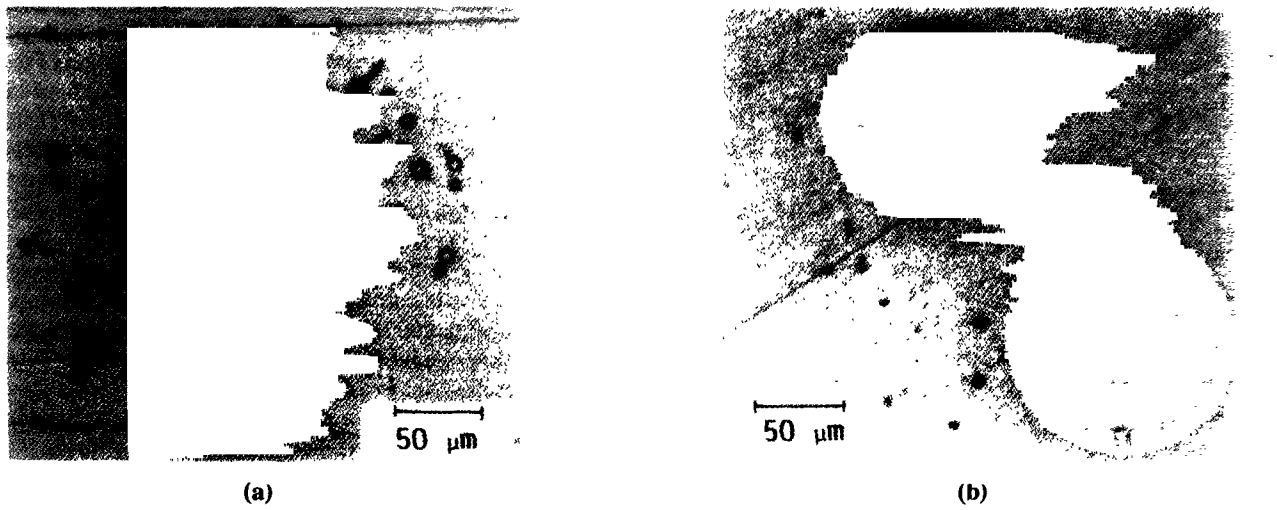

Fig 6. Alumina splats collected on a steel substrate for particles sprayed with the rf plasma torch. (a) Substrate at 75 °C. (b) Substrate at 300 °C

the relaxation of the quenching stresses (Ref 18) within the splats depends strongly on this contact and on the splat cooling rate. Zirconia particles sprayed with either dc or rf torches are well melted at impact ($T > 3600$ K), zirconia being easier to melt than alumina. Thus, the microcrack network is more dense for particles impacting at high velocity (≈220 m/s when sprayed with the 7 mm ID nozzle dc plasma torch) compared to those impacting at low velocity (≈30 m/s when sprayed with the rf plasma torch). When spraying alumina, the phenomenon is reversed. As the particles achieve higher temperatures, $T > 3800$ K with the rf plasma torch, compared to 2800 K with the 7 mm ID nozzle dc torch), adhesion to the substrate improves for the rf-sprayed particles. In this case the microcrack network is less dense within the splats obtained with the 7 mm ID nozzle plasma torch (Fig. 4b) than in those obtained with the rf plasma torch (Fig. 6b).

Table 2 summarizes alumina particle velocity and surface temperature at impact for the three torches. For dc spraying, particle velocity was measured by laser Doppler anemometry (LDA) and particle surface temperature by fast (response time of about 0.1 μs) two-color pyrometry (Ref 19). For rf plasma spraying, mean particle velocity and temperature (assumed to be uniform) were calculated by Proulx (Ref 20) for the -90+45 μm

Table 1 Average alumina splat parameters obtained with dc and rf torches (a)

Torch	Shape factor (b)	Diameter (b), μm	Thickness, μm	Flattening degree(c)
7 mm ID dc	0.92 ± 0.12	90 ± 28	1.1	4.8
rf plasma	0.97 ± 0.07	88 ± 26	2.3	3.85

(a) – 45 ± 22 μm particle size. (b) The mean value and standard deviation were obtained with about 250 splats. (c) The flattening degree is a dimensionless unit equal to D/d, where D is splat diameter (assumed to be a disk) (μm) and d is in-flight particle diameter (assumed to be spherical) (μm).

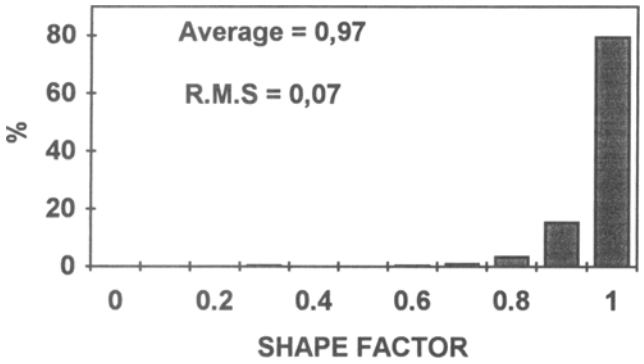

Fig 7 Shape factor distribution for alumina splats on a steel substrate at 300 °C for particles sprayed with the rf plasma torch

Table 2 Parameters for alumina particles at impact

Torch	Particle velocity, m/s	Particle temperature, K
-90+45 μm particles		
7 mm ID dc	130 ± 10	2800 ± 250
10 mm ID dc	90 ± 8	2700 ± 250
rf plasma	45	3800
-45+22 μm particles		
7 mm ID dc	250 ± 10	2800 ± 250
10 mm ID dc	130 ± 10	2650 ± 250

size distribution. However, according to results obtained with the dc torches, it can reasonably be assumed that the small particle temperature is higher than the large particle temperature. The calculated particle temperature for the IPS process was higher than that measured for APS. Such high values are confirmed by the measurement of the in-flight particle surface temperature by Takikawa et al. (Ref 21), who measured 3000 K with a pure argon plasma of 15 kW.

Table 3 summarizes the results for -90+45 μm alumina particles sprayed with the 10 mm ID dc torch and the rf plasma torch. The flattening degrees obtained with both torches were about the same, despite the lower velocity of the rf plasma torch compared to the dc torch (45 versus 130 m/s). Thus, the rf plasma torch affords improved melting of large particles.

3.1.2 Sandblasted Stainless Steel Substrates ($R_a \approx 3$ μm)

Flattening is quite different on rough substrates, at least in the case of molybdenum particles (Ref 22). Figures 8(a) and (b) show alumina splats collected on sandblasted ($R_a \approx 3$ μm) type 304L stainless steel substrates at either 75 or 300 °C. The micrographs were obtained using the backscattered electron technique.

Splats were not as lenticular (Fig. 8b) on hot (300 °C) rough substrates as on smooth ones, but the same general tendency was observed. Each splat was rather compact with a few pores (probably due to the escape of the gas entrapped within the asperities beneath it). The microcrack network appeared to be less dense compared to materials sprayed onto flat substrates. This was probably due to the thicker splat and to the fact that a rough substrate can better accommodate strains, the flow of the material being limited by surface asperities.

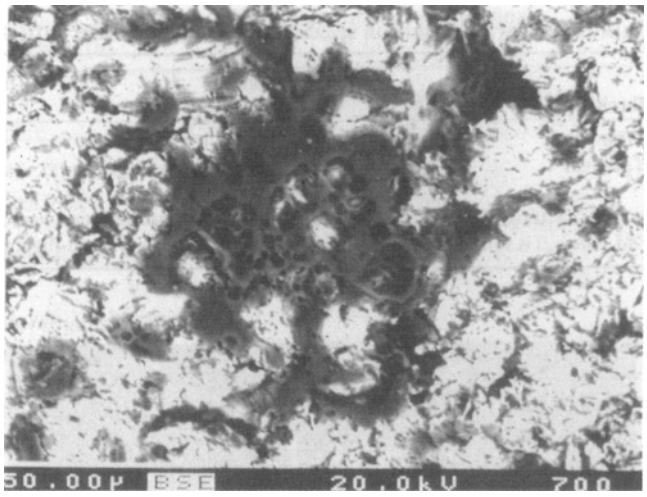

(a)

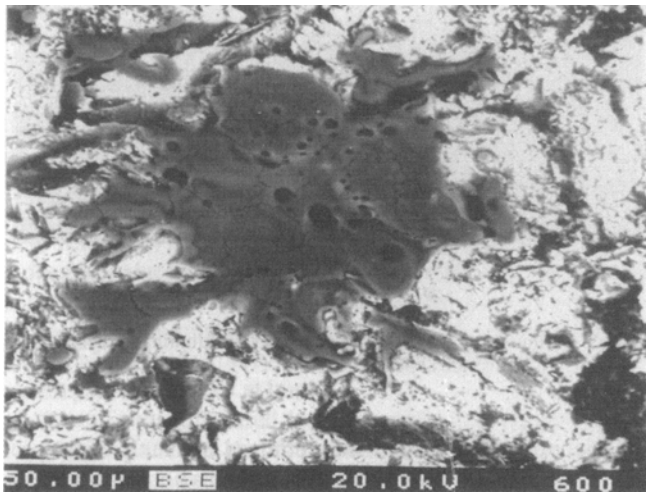

(b)

Fig 8. Alumina splats obtained on a rough stainless steel substrate ($R_a = 3$ μm) for particles sprayed with the 7 mm ID nozzle dc plasma torch. (a) Substrate at 75 °C. (b) Substrate at 300 °C

Splats were more distorted on cold substrates (75 °C) (see Fig. 8a) than those collected on hot substrates and exhibited a lack of material at the splat center. Material apparently splashes away, probably because of poor contact with the substrate and the extended cooling time. Although splats on rough substrates are quite different from those collected on smooth substrates, the same general tendencies can be observed.

3.1.3 Alumina-Sprayed Polished Substrates ($R_a \approx 0.4$ μm)

Spraying onto alumina-sprayed polished samples (>97% γAl_2O_3) results in a splat morphology identical to that obtained on polished stainless steel substrates. In the case of the 7 mm ID nozzle dc plasma torch, the splats collected with a low surface temperature (Fig. 9a) were very distorted in shape and had poor

Table 3 Average alumina splat parameters obtained with dc and rf torches (a)

Torch	Shape factor (b)	Diameter (b), μm	Thickness, μm	Flattening degree (c)
10 mm ID dc	0.94 ± 0.13	171 ± 66	2.9	4.3
rf plasma	0.98 ± 0.04	164 ± 64	3.3	4.1

(a) –90+45 μm particle size. (b) The mean value and standard deviation were obtained with about 250 splats. (c) The flattening degree is a dimensionless unit equal to D/d, where D is splat diameter (assumed to be a disk) (μm) and d is in-flight particle diameter (assumed to be spherical) (μm).

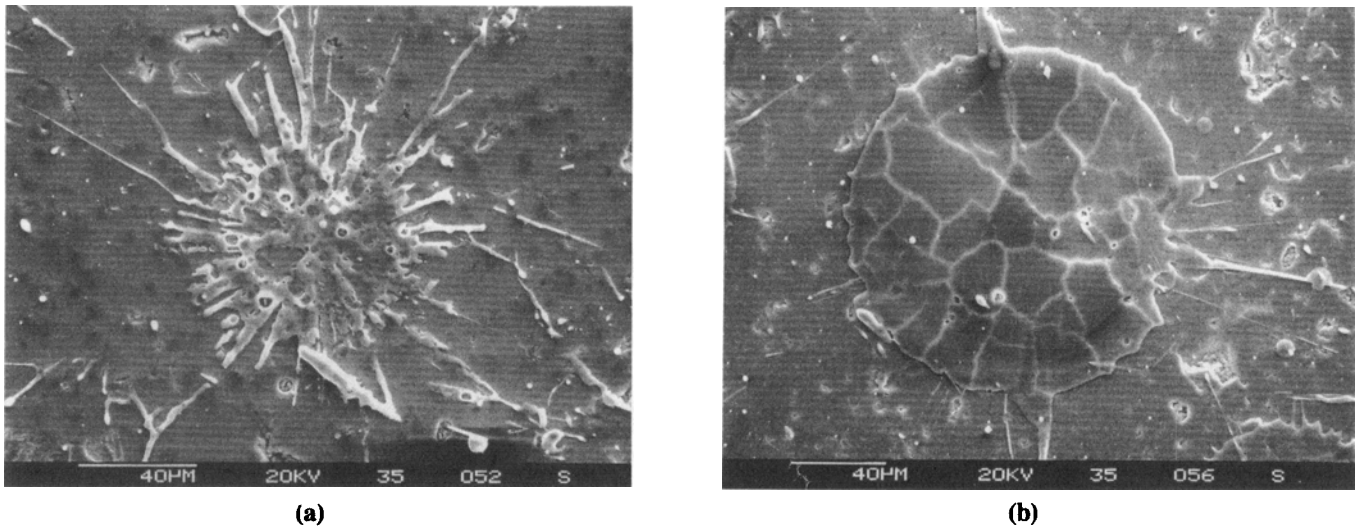

(a) (b)

Fig 9. Alumina splats collected on a polished alumina-sprayed substrate for particles sprayed with the 7 mm ID nozzle dc plasma torch. (a) Substrate at 75 °C. (b) Substrate at 500 °C

adhesion to the substrate (being removed by the tip of the profilometer). However, the splats obtained on a hot substrate (Fig. 9b) were nearly perfect disks with good substrate contact as confirmed by the microcrack network. The study of splats collected on rough alumina substrates is difficult because of poor contrast, but it can reasonably be assumed that their behavior is much the same as on smooth substrates.

3.2 *Study of Alumina Deposits Sprayed with or without Preheating of the Substrate*

3.2.1 Deposit Microstructure

The fracture SEM micrograph of an alumina deposit sprayed with the rf plasma torch (Fig. 10a) shows a columnar growth structure. Many investigators (Ref 10, 23, 24) have noticed this structure on plasma-sprayed alumina coatings despite high particle cooling rates, which according to these researchers should produce high undercooling and result in homogeneous nucleation. In the case of zirconia particles (Ref 17), this cooling rate, at the start of splat cooling, can exceed 4×10^8 K/s and more generally ranges from 10^6 to 10^8 K/s. Such cooling rates for individual splats of either zirconia or alumina collected on smooth substrates at 300 °C have led to columnar growth distributed over the entire splat surface, regardless of impact particle velocity. Moreover, under these conditions, this columnar growth seems to develop within a pass consisting of three or five piled splats, as shown in Fig. 10. In Fig. 10(b), individual splats 2 to 3 μm thick are still visible on the deposit, probably due to the fracture mechanisms, confirming the values obtained with rf spraying (see Table 1).

3.2.2 Coating Properties

The deposits obtained under different spraying conditions were dense, with less than 6% open porosity. No significant variations occurred between the deposits built up with the two powder size distributions. It should be emphasized, however, that large particles (–90+45 μm) were not sprayed with the 7 mm ID nozzle plasma torch; this would have produced more unmolten particles due to their shorter residence time in the plasma jet.

Adhesion tests were performed for each condition with substrates either preheated to 300 °C or kept at room temperature prior to spraying (see Fig. 2). During spraying on a substrate preheated to 300 °C, the heat released by the impacting particles increased the temperature by about 50 °C a few seconds after the start of powder injection. During spraying on a cold substrate (with the same cooling conditions as for preheated substrates), the surface temperature increased progressively to about 350 °C for a 0.3 mm thick coating. Considering Fig. 2, it is clear that for the first 0.1 mm of the coating the temperature of the substrate

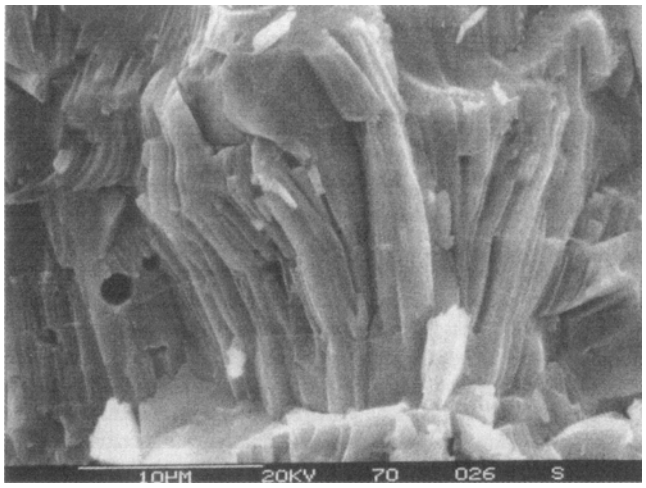

(a)

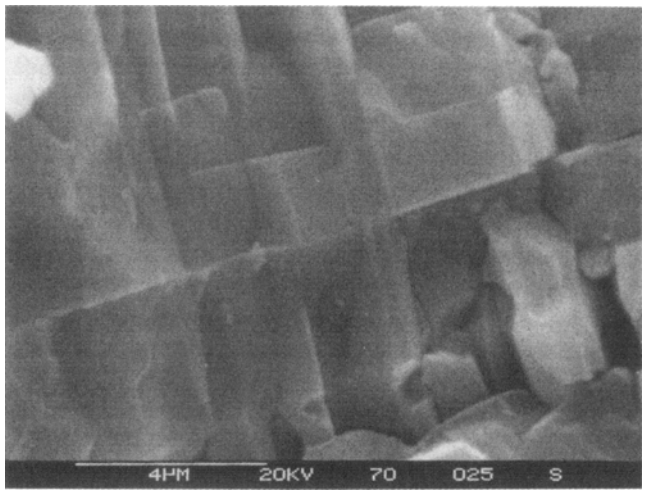

(b)

Fig. 10 SEM fracture micrographs of an IPS alumina coating. (a) Columnar growth structure. (b) Individual splats visible on the deposit

and previously deposited layers was below 200 °C, resulting in poor contact between the splats.

Table 4 shows the results of adhesion and microhardness testing of the alumina deposits. Preheating the substrate prior to spraying always induces higher values of coating adhesion regardless of particle size and plasma parameters. This phenomenon is probably linked to the difference in splat morphologies with respect to the substrate temperature. Thus, when the substrate is kept at room temperature (and, more generally, below 100 °C), the splats are extensively fingered and, according to their low cooling rates (Ref 14), have very poor contact with the substrate or the previously deposited layers. Moreover, without preheating, the stresses due to temperature gradients must be added to those resulting from the expansion coefficient mismatch ($\Delta\alpha = 7 \times 10^{-6}$ m/m · K). These stresses will be relaxed by macrocracks, which contribute to the poor contact between the lamellae and to the reduction of coating adhesion values.

When the substrate is preheated to temperatures greater than 300 °C before spraying, contact of the splats to the substrate or

Table 4 Adhesion and microhardness of alumina coatings (a)

Torch	Preheating	Hardness, HV (5N)	Adhesion, MPa
–45+22 μm particles			
7 mm ID dc	No	972 ± 76	15 ± 2
	Yes	1091 ± 115	34 ± 2
10 mm ID dc	No	908 ± 66	15 ± 2
	Yes	799 ± 130	24 ± 2
–90+45 μm particles			
10 mm ID dc	No	633 ± 11	5 ± 1
	Yes	758 ± 107	10 ± 2
rf plasma	No	980 ± 93	12 ± 2
	Yes	1110 ± 122	21 ± 3

(a) All failures occurred at the substrate/coating interface.

previously deposited alumina layers is good (i.e., high cooling rates occur), probably due to increased wettability of the ceramic droplets.

The strong influence of particle velocity on splat contact with the hot substrates (their cooling rates increase when their velocity at impact increases) has already been noted. A corresponding improvement of coating adhesion for –45+22 μm particles on preheated substrates also occurs when sprayed with a mean particle velocity (v) of about 250 m/s compared to a v of 130 m/s. Adhesion values are quite similar for deposits on nonpreheated substrates, regardless of v at impact. In this case, the poor contact between the splats and the substrate or previously deposited layers, which leads to very distorted splats, is no longer dependent on particle velocity at impact.

Coatings manufactured from the –90+45 μm feedstock exhibit lower adhesion than those formed from smaller-particle –45+22 μm feedstock, regardless of substrate temperature. This is probably due to the better melting of smaller particles. With IPS, particle residence times are commonly ten times longer than in a conventional plasma jet. Thus, the improvement in the adhesion of IPS alumina coatings compared to that of APS coatings is due to better particle melting. Adhesion values for IPS alumina coatings are twice those of APS coatings (Table 2).

Interpretation of the hardness values is more difficult. However, two conclusions can be drawn:

- Coatings sprayed at 300 °C are generally harder than those sprayed at less than 100 °C.
- For the same particle size distribution, coatings sprayed at higher velocities exhibited higher hardnesses, except when the particles were not well melted.

4. Conclusion

Alumina particle flattening was investigated for different substrates using a setup derived from the line scan test. Three torches were used to vary particle velocity from 60 to 250 m/s for –45+22 μm fused and crushed particles. Splats exhibited two morphologies that depended only on substrate temperature and oxidation rate. When particles were sprayed onto a polished

stainless steel substrate and a polished alumina-sprayed substrate kept at a temperature of 300 °C, the splats were nearly disk-shaped and their contact with the substrate was very good, according to the measured high cooling rate values. If the same substrates were kept at room temperature prior to spraying (below 100 °C) and/or if the oxide layer on the substrate (hot or cold) was too thick, very distorted and extensively fingered splats resulted. These splats adhered poorly to the substrate and showed low cooling rates. Use of rough stainless steel substrates resulted in the same general behavior.

In order to correlate these results with coating properties, deposits were formed under the same conditions with careful control of the substrate and coating temperatures during spraying. Adhesion testing of the deposits confirmed the results obtained on individual splats; higher values resulted when the substrate was preheated to 300 °C prior to spraying. Better melting of larger particles (–90+45 μm) occurred with the rf plasma torch than with the 10 mm ID nozzle dc torch, leading to higher values of adhesion. Adhesion of deposits on hot substrates increased with particle velocity at impact, as long as the particles were well molten. Preheating the substrate to temperatures greater than 200 °C prior to spraying improved deposit adhesion, provided that the oxidation of the substrate remained constant.

References

1. P. Fauchais, J.F. Coudert, M. Vardelle, A. Vardelle, and A. Denoirjean, Diagnostics of Thermal Spraying Plasma Jets, *J. Therm. Spray Technol.*, Vol 1 (No. 2), 1992, p 117-128
2. M.I. Boulos, R.F. Induction Plasma Spraying: State-of-the-Art Review, *J. Therm. Spray Technol.*, Vol 1 (No. 1), 1992, p 33-40
3. M. Vardelle, A. Vardelle, and P. Fauchais, Spray Parameters and Particle Behavior Relationships during Plasma Spraying, *J. Therm. Spray Technol.*, Vol 2 (No. 1), 1993, p 79-91
4. W.D. Swank, J.R. Fincke, and D.C. Haggard, Behavior of Ni-Al Particles in Argon:Helium Plasma Jets, *J. Therm. Spray Technol.*, Vol 2 (No. 3), 1993, p 243-249
5. S.J. Yankee and B.J. Pletka, Effect of Plasma Spray Processing Variations on Particle Melting and Splat Spreading of Hydroxylapatite and Alumina, *J. Therm. Spray Technol.*, Vol 2 (No. 3), 1993, p 272-281
6. S. Fantassi, M. Vardelle, A. Vardelle, and P. Fauchais, Influence of the Velocity of Plasma Sprayed Particles on Splat Formation, *J. Therm. Spray Technol.*, Vol 2 (No. 4), 1993, p 379-384
7. C. Berndt et al., Current Problems in Plasma Spray Processing, *J. Thermal Spray Technol.*, Vol 1 (No. 4), 1992, p 341-356
8. S. Safai and H. Herman, Microstructural Investigation of Plasma Sprayed Aluminium Coatings, *Thin Solid Films*, Vol 45, 1977, p 295-307
9. S. Sampath, "Rapid Solidification during Plasma Spraying," Ph.D. thesis, SUNY at Stony Brook, Aug 1989
10. R. McPherson, The Relationship between the Mechanism of Formation, Microstructure and Properties of Plasma Sprayed Coatings, *Thin Solid Films*, Vol 83, 1981, p 297-310
11. K.A. Roberts and T.W. Clyne, A Simple Procedure for the Characterization of Spray Deposition—The Line Scan Test, *Surf. Coat. Technol.*, Vol 41, 1990, p 103-115
12. M.P. Planche, O. Betoule, J.F. Coudert, A. Grimaud, M. Vardelle, and P. Fauchais, Performance Characteristics of a Low Velocity Plasma Spray Torch, *Thermal Spray Coatings: Research Design Applications*, C.C. Berndt and T.F. Bernecki, Ed., ASM International, 1993, p 81-87
13. J. Jurewicz and M.I. Boulos, High Energy Density Induction Plasma System for Materials Processing, *Thermal Spray Coatings : Research Design Applications*, C.C. Berndt and T.F. Bernecki, Ed., ASM International, 1993, p 89-95
14. L. Bianchi, M. Vardelle, A. Vardelle, F. Blein, P. Lucchèse, and P. Fauchais, Effect of Particle Velocity and Substrate Temperature on Alumina and Zirconia Splat Formation, *Thermal Spray: Industrial Applications*, C.C. Berndt and S. Sampath, Ed., ASM International, 1994, p 569-574
15. L. Bianchi, A. Grimaud, F. Blein, P. Lucchèse, and P. Fauchais, Comparison of Plasma Sprayed Alumina and Zirconia Coatings by r.f. and d.c. Plasma Spraying, *Thermal Spray: Industrial Applications*, C.C. Berndt and S. Sampath, Ed., ASM International, 1994, p 575-579
16. L. Bianchi, M. Mellali, A. Grimaud, P. Lucchèse, and P. Fauchais, How to Control Substrate and Coating Temperature during Spraying to Enhance the Adhesion of Alumina Coatings, *ISPC 11 Proc.*, Vol 1, J. Harry, Ed., University of Loughborough, U.K., 1993, p 172-177
17. M. Vardelle, A. Vardelle, A.C. Leger, P. Fauchais, and D. Godin, Influence of the Particle Parameters at Impact on Splat Formation and Solidification in Plasma Spraying Processes, *J. Therm. Spray Technol.*, to be published
18. S. Kuroda, T. Fukushima, and S. Kitahara, Significance of Quenching Stress in the Cohesion and Adhesion of Thermally Sprayed Coatings, *J. Therm. Spray Technol.*, Vol 1 (No. 4), 1992, p 325-332
19. M. Vardelle, A. Vardelle, P. Fauchais, and C. Moreau, Pyrometer System for Monitoring the Particle Impact on a Substrate during Plasma Spray Process, *Meas. Sci. Technol.*, Vol 5, 1994
20. P. Proulx, Ph.D. thesis, University of Sherbrooke, Quebec, Canada, 1987
21. H. Takikawa, T. Sakuta, and M. I. Boulos, In-Flight Measurement of Particle Velocity and Surface Temperature in an Inductively Coupled R.F. Plasma, *ISPC 9 Proc.*, Vol 1, R. d'Agostino, Ed., University of Bari, Italy, 1989, p 371-376
22. C. Moreau, P. Gougeon, and M. Lamontagne, Influence of the Substrate Preparation on the Flattening and Cooling of Plasma Sprayed Particles, *J. Therm. Spray Technol.*, to be published
23. R. McPherson, On the Formation of Thermally Sprayed Alumina Coatings, *J. Mater. Sci.*, Vol 8, 1973, p 851-858
24. G.N. Heintze and S. Uematsu, Preparation and Structures of Plasma-Sprayed γ and α-Al_2O_3 Coatings, *Surf. Coat. Technol.*, Vol 50, 1992, p 213-222